

A NEW TECHNIQUE FOR THE FATIGUE LIFE PREDICTION IN NOTCHED COMPONENTS

Thibault Herbland^{a,b}, Georges Cailletaud^b, Stephane Quilici^b, Haïdar Jaffal^a

^aCetim, Senlis, France

^bCentre des Matériaux, MINES-ParisTech, CNRS UMR 7633, 91003 Evry Cedex, France

Abstract After pointing out the limitations of the classical Neuber type methods, we propose a new procedure for calculating fatigue life of notched components. It includes a new approach for accelerated evaluation of stress and strain histories at the notch tip. A methodology coming from the study of uniform fields models is used to describe the evolution of the residual stresses at the notch tip. A tensorial variable allows us to take into account the stress redistribution around the notch tip. The model is calibrated by two short FEM computations of the component representing a monotonic preload of the structure, first with the elastic behaviour, then with the real elasto-plastic behaviour. These computation results are used to determine the parameters of the transition rule, which allows to simulate the whole loading history. The local stress histories are then treated through a new multiaxial rainflow cycle counting algorithm. Contrary to classical rainflow algorithms that count an equivalent variable, it takes into account the whole stress tensor. First, a new algorithm is used to determine the minimum circle circumscribed to the deviatoric load path. Then, cycles are extracted following the "active surfaces" concept used in some plasticity models. Then, the multiaxial Chaboche model is applied to compute the elementary damage generated by each extracted cycle. Finally, a non-linear cumulation rule is used to achieve the total damage generated by a load sequence, and the fatigue life of the component. The full method was successfully applied to several notch geometries of components subjected to different loadings, with cyclic or random load paths.

1 INTRODUCTION

To predict the fatigue life of a component, we need to determine the local variables at the critical point (i.e. the notch tip). This can be done by means of a finite element method (FEM) computation, but it is time consuming, especially when complex structures are subjected to low cycle fatigue. That is why engineers often use accelerated computation methods. Some of them directly determine the stabilized values of stresses and strains over the whole structure. These methods do not provide any information on the accommodation process. Other methods compute the values of stresses and strains only at the critical point, but during the whole history. The well-known Neuber method [17] was the first one ever developed for uniaxial stress states. Many researchers tried to extend this method to multiaxial stress states [11] [1] [16] but at this day, no method can accurately compute local variables. The far most efficient method is the Buczynski-Glinka's one [5], but it still fails to predict for example the hoop stress and strain on an axisymmetric notched specimen. In this paper we address Neuber-type methods. The new presented approach is based on an adjustable scale transition rule that was originally dedicated to micro-macro modelling of polycrystals [6, 7]. But here we consider the material element at the notch root as a plastic inclusion in an elastic matrix playing the role of an homogeneous medium. The model was validated on many loading cases, here we will present the most complex one: a multiaxial random non-proportional tension-torsion loading. After that, a multiaxial rainflow cycle counting algorithm and a 3D-Lemaitre-Chaboche damage law will be used to predict fatigue life. Results provided by a reference FEA will be used as a reference for our method.

2 MODEL DESCRIPTION

2.1 Model background

Using the solution of the problem of a spherical inclusion I in an infinite matrix M , Kröner's model allows to determine the relation between the average stress tensor ($\underline{\sigma}^M$), the stress tensor in an inclusion of an aggregate ($\underline{\sigma}^I$), the average plastic strain tensor ($\underline{\xi}^{pM}$) and the plastic strain tensor in the inclusion ($\underline{\xi}^{pI}$) [12]. The theory is based on Eshelby's solution of an inclusion in an infinite matrix, whose behaviour is supposed to remain elastic:

$$\underline{\sigma}^I = \underline{\sigma}^M + \underline{C} : (\underline{\xi}^{pM} - \underline{\xi}^{pI}) \quad (1)$$

The fourth order tensor \underline{C} depends on the elastic properties and of the shape of the inclusions. As classically shown [2], this linear correction involves an elastic accommodation, so that the residual stresses (*id est* the difference between the average stress and the stress in the inclusion) are too large. The residual stress level is valid at the onset of plastic deformation in the inclusion, nevertheless, a more realistic evaluation for larger plastic strains must involve a plastic accommodation. This is the case in the self-consistent approach developed by Hill [10], and also in the “ β -rule” proposed by Cailletaud and Pilvin [6, 7]. The interest of this last model is to combine an explicit formulation and a plastic accommodation. The idea is just to replace the plastic strain $\underline{\xi}^{pI}$ in eq. 2 by an auxiliary variable, $\underline{\beta}^I$, with a non linear evolution, so that the amount of residual stress is limited. The average of $\underline{\beta}^I$ on the whole aggregate is $\underline{\beta}$, and the model writes now:

$$\underline{\sigma}^I = \underline{\sigma}^M + \underline{C} : (\underline{\beta} - \underline{\beta}^I) \quad \text{with} \quad \dot{\underline{\beta}}^I = \dot{\underline{\xi}}^{pI} - \underline{D} : \underline{\beta}^I \|\dot{\underline{\xi}}^{pI}\| \quad (2)$$

2.2 The new models

Two types of corrections will be introduced, by adapting the two previously presented methods for the case of the material element located at the notch tip. It will be assumed that stresses and strains concentrate in this area, and that the redistribution observed is similar to the stress and strain evolution in an inclusion. An important modification has to be made in the corrective term: since the material element is at the surface, three components of the stress tensor must remain equal to zero.

The linear correction (L-type) writes:

$$\underline{\sigma}^I = \underline{\sigma}^M + \underline{C}^L : (\underline{\xi}^{pM} - \underline{\xi}^{pI}) \quad (3)$$

Assuming that the normal to the free surface is x_1 , three lines and three columns of the \underline{C}^L tensor must be full of zeros. On the other hand, $\underline{\xi}^{pM}$ is negligible since the global plasticity remains small.

The non-linear correction (N-type) writes:

$$\underline{\sigma}^I = \underline{\sigma}^M + \underline{C}^N : (\underline{\beta} - \underline{\beta}^I) \quad \text{with} \quad \dot{\underline{\beta}}^I = \dot{\underline{\xi}}^{pI} - \underline{D}^N : \underline{\beta}^I \|\dot{\underline{\xi}}^{pI}\| \quad (4)$$

Again, \underline{C}^N and \underline{D}^N tensors have zeros on three columns and three lines. In equations 3 and 4, $\underline{\sigma}^I$ and $\underline{\xi}^{pI}$ characterize now the stress and plastic strain tensor at the notch tip, meanwhile $\underline{\sigma}^M$ is the uncorrected reference stress. The equivalent average tensor $\underline{\beta}$ is negligible.

Unlike Kröner's or Hill's models, this approach has adjustable parameters. The tensor component must be customized to take into account various types of materials (see for instance an application to directionnally solidified alloys in [19]). The purpose of the present paper is to investigate the calibration of the model for a finite body with a free surface. The plastic zone at

the notch tip is considered as a specific inclusion, and the zone surrounding this material element plays the role of the equivalent medium. It is worth mentioning that the analogy between this case and the class of theories used for the definition of homogenization models is not fully verified. Inclusions in infinite media are submitted to an uniform state of stress. This is no longer the case for the material element of the notch root, since the reference medium is a finite specimen, and a free surface is introduced.

In the case of the N-type correction for example, the fourth order tensors $\underset{\approx}{C}^N$, $\underset{\approx}{D}^N$ have to be determined from FEA. For a tension-torsion loading on the longitudinal axis $\hat{2}$ of a notched axisymmetric specimen, the shape of these tensors is the following in Voigt notation (with $(1, 2, 3) \equiv (r, z, \theta)$):

$$\underline{\sigma} \equiv \begin{pmatrix} 0 \\ \sigma_2 \\ \sigma_3 \\ 0 \\ \sigma_5 \\ 0 \end{pmatrix} \quad \underline{\varepsilon} \equiv \begin{pmatrix} \varepsilon_1 \\ \varepsilon_2 \\ \varepsilon_3 \\ 0 \\ \varepsilon_5 \\ 0 \end{pmatrix} \quad (5)$$

Three lines and three columns in $\underset{\approx}{C}^N$ and $\underset{\approx}{D}^N$ are then full of zeros to ensure a zero stress vector at the free surface. $\underset{\approx}{C}^N$ and $\underset{\approx}{D}^N$ are symmetrical.

$$\underset{\approx}{C}^N \equiv \begin{pmatrix} 0 & 0 & 0 & 0 & 0 & 0 \\ 0 & C_{22}^N & C_{23}^N & 0 & 0 & 0 \\ 0 & C_{23}^N & C_{33}^N & 0 & 0 & 0 \\ 0 & 0 & 0 & 0 & 0 & 0 \\ 0 & 0 & 0 & 0 & C_{55}^N & 0 \\ 0 & 0 & 0 & 0 & 0 & 0 \end{pmatrix} \quad \underset{\approx}{D}^N \equiv \begin{pmatrix} 0 & 0 & 0 & 0 & 0 & 0 \\ 0 & D_{22}^N & D_{23}^N & 0 & 0 & 0 \\ 0 & D_{23}^N & D_{33}^N & 0 & 0 & 0 \\ 0 & 0 & 0 & 0 & 0 & 0 \\ 0 & 0 & 0 & 0 & D_{55}^N & 0 \\ 0 & 0 & 0 & 0 & 0 & 0 \end{pmatrix} \quad (6)$$

These tensors are introduced in eq. 4, where the macroscopic plastic strain tensor has been set to zero, and the local plastic strain is replaced by $\underline{\beta}^I$:

$$\underline{\sigma}^I = \underline{\sigma}^M - \underset{\approx}{C}^N : \underline{\beta}^I \quad (7)$$

Eight correction rule parameters have to be calibrated, four in $\underset{\approx}{C}^N$, four in $\underset{\approx}{D}^N$. For this purpose, we use an optimization procedure. This algorithm takes the results of two FE computations as target solutions, and the result of the accelerated computation:

- an elastic computation of the structure, to evaluate the elastic stress state at the notch root for a monotonic loading;
- an elasto-plastic computation, providing the evolution of the local stresses and strains during the same loading. This solution is considered as a reference.

The constitutive equations are obtained by introducing the von Mises plasticity criterion, a plastic flow rate deduced from the normality rule, and a non-linear kinematic behaviour [13]:

$$f(\underline{\sigma}) = J(\underline{\sigma} - \underline{\mathbf{X}}) - R_0 \quad \text{with} \quad J(\underline{\sigma}) = ((3/2) s_{ij} s_{ij})^{1/2} \quad (8)$$

$$\dot{\underline{\varepsilon}}^p = \dot{p} \frac{\partial f}{\partial \underline{\sigma}} \quad (9)$$

\dot{p} is evaluated in the consistency condition. At constant temperature, the evolution rule for kinematic hardening is:

$$\dot{\underline{\mathbf{X}}} = \frac{2}{3}C\dot{\underline{\underline{\xi}}}^p - D\underline{\underline{\mathbf{X}}}\dot{p} \quad (10)$$

We first test the effect of the nature of the correction, by using a plate specimen subjected to tensile loading, thus resulting in an uniaxial stress state at the notch tip. Then, 30 cycles are simulated with the same parameters. Whereas we reach a mechanical steady state for the L-type correction, the mechanical response for the N-type correction exhibits an unlimited ratchetting effect. This last behaviour is unrealistic: it is neither observed during experimental tests nor in finite elements analysis in the case of confined plasticity: even if the loading is stress-controlled, strains are constrained by the elastic matrix surrounding the notch tip, and the local load is strain-controlled. This effect is only due to the non-linearity of the correction rule: such a behaviour is classically obtained with the Chaboche-type constitutive equations, when a representative volume element (RVE) is subjected to a repeated loading under stress control. To avoid this unrealistic ratchet, one often superposes a linear kinematic hardening to the non-linear one. In the present case, we derive a new expression for our correction term:

$$\dot{\underline{\underline{\beta}}}^I = \dot{\underline{\underline{\xi}}}^{pI} - D_{\underline{\underline{\beta}}}^N : \left(\underline{\underline{\beta}}^I - \underline{\underline{\delta}} : \underline{\underline{\xi}}^{pI} \right) \|\dot{\underline{\underline{\xi}}}^{pI}\| \quad (11)$$

The tensor $\underline{\underline{\delta}}$ is just a diagonal, and we observed that the values of the components related to torsion were half of the ones related to tension. This ninth parameter has to be calibrated over 3 branches of a repeated loading. For the applications that are shown in the following, we observed that L-type correction gives a good accuracy when applied to constant-amplitude loadings. This is an interesting result, since the number of parameters that have to be calibrated is rather low. However, in the case of variable-amplitude loadings, the N-type correction appears to be far more accurate. Thus we decided to use the L-type correction in case of constant-amplitude loadings, and the N-type correction for variable-amplitude loadings.

3 FATIGUE LIFE PREDICTION

3.1 Multiaxial rainflow algorithm

This algorithm was developed by Melnikov and Semenov [15] and implemented in ZeBuLoN code by Quilici and Musienko [18]. Starting from the loading path, it provides a series of centers and ranges that characterize the cycles. It is based on the ‘‘active surface’’ concept used in some plasticity models, and on a cycle extraction procedure inspired from the uniaxial rainflow technique. There is no threshold in the model.

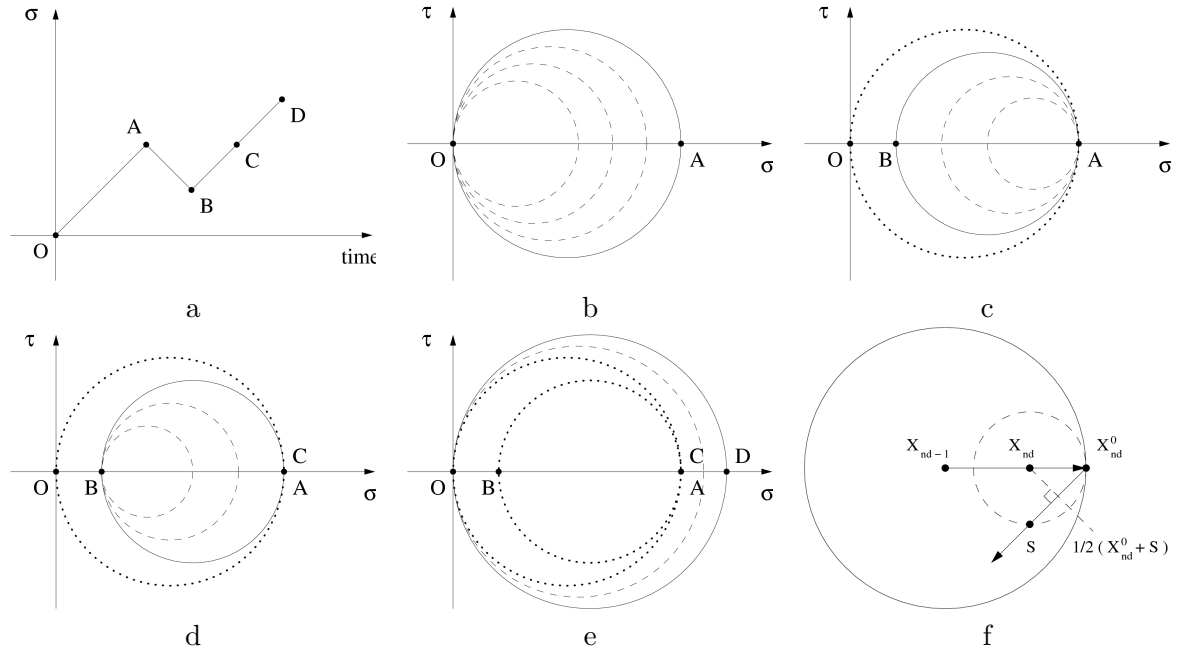


Figure 1: Illustration of the cycle extraction procedure: (a) Example of a one dimensional loading path; (b) Successive locations (dashed circles) of the domain circumscribing the loading path during the first loading OA and final position (solid circle); (c) Successive locations and final domains during AB branch (d) Successive locations and final domains during BC branch (e) Elimination of the circle of diameter AB and growth of the former OA diameter circle to reach OD. (f) Determination of the center of the current active surface for a non-proportional loading [18]

The various steps of the algorithm used for cycle extraction are given in figure 1. A simple loading path for a one dimensional tensile loading (figure 1 (a)) is taken as an example. The algorithm starts with a circle reduced to a point in O. During the first branch OA, the diameter increases to remain equal to the actual load, so that the final position corresponds to a circle of diameter OA (figure 1 (b)). Just after A, following the AB branch, an unloading is detected, and a new active surface is created, whose final size corresponds to a diameter AB (figure 1 (c)). A new unloading is detected after B along BC branch, and new active surfaces are created inside the (AB) circle. Once the current point reaches C, the second and the third active surfaces coincide, that means that one cycle is closed, and it is extracted (figure 1 (d)). After extraction, only the initial circle of diameter OA remains in the plane. It is reactivated and keeps growing until point D is reached (figure 1 (e)).

In this 1D case, unloading is easy to detect, however in more complex cases a criterion is needed. This is illustrated in figure 1 (f), where it is assumed that a solid-line surface defined by its center ($\tilde{\mathbf{X}}_{nd-1}$) and its radius R has been created. After this point, the unloading condition writes:

$$(\tilde{\mathbf{S}} - \tilde{\mathbf{X}}_{nd-1}) : d\tilde{\mathbf{S}} < 0 \quad (12)$$

When unloading is detected, the origin $\tilde{\mathbf{X}}_{nd}^0$ of the new active surface is saved. Then, the center $\tilde{\mathbf{X}}_{nd}$ of this surface moves between $\tilde{\mathbf{X}}_{nd}^0$ and the center of the former active surface $\tilde{\mathbf{X}}_{nd-1}$. This center is the intersection of the right bisector of (S, X_{nd}^0) at point $\frac{1}{2}(X_{nd}^0 + S)$ with the straight line (X_{nd-1}, X_{nd}^0) .

3.2 Lemaitre-Chaboche damage law

In this paper we use the classical Lemaitre-Chaboche damage law for multiaxial stress states [14], [13]. This model introduces a non-linear damage cumulation rule, expressed by a differential equation:

$$dD = \left(1 - (1 - D)^{\beta+1}\right)^{\alpha(\Delta J, \bar{I}_1, J_{max})} \left(\frac{\Delta J/2}{M(\bar{I}_1)}\right)^{\beta} dN \quad (13)$$

where ΔJ is the diameter of the circle circumscribed to the loading space in the deviatoric stress space [4], \bar{I}_1 is the mean value of the first stress invariant and J_{max} the maximum value of the von Mises invariant of the stress tensor.

The function $\alpha(\Delta J, \bar{I}_1, J_{max})$ characterizes the non-linearity of the damage evolution, defines the non-linear cumulation, and allows to take into account the mean stress effect:

$$\alpha(\Delta J, \bar{I}_1, J_{max}) = 1 - a \left\langle \frac{\Delta J/2 - \sigma_l(\bar{I}_1)}{\sigma_u - J_{max}} \right\rangle \quad (14)$$

where $\sigma_l(\bar{I}_1) = \sigma_{l0} (1 - 3 \bar{I}_1 / \sigma_u)$

The expression of $M(\bar{I}_1)$ is derived from Gerber's uniaxial fatigue criterion and induces a mean stress effect again:

$$M(\bar{I}_1) = \sigma_{l0} \left(1 - 3 \frac{\bar{I}_1}{\sigma_u}\right) \quad (15)$$

4 COMPARISON BETWEEN THE MODEL PREDICTIONS AND REFERENCE FEA

The validation of the present method is now made by comparing the results of our model to those provided by a finite element analysis considered as a reference. An axisymmetrical notched specimen is computed with the code ZSeT/ZeBuLoN [3]. This geometry is critical for most of the other models. In particular, the hoop stress and strain are generally not well captured.

The core diameter is 9.2 mm; the diameter at the notch root is 7 mm. The radius of the notch is 0.4 mm. The stress concentration factor in tension (σ_2 at the notch root divided by σ_2 on the top of the specimen) is 2.7; the same ratio computed for the case of a torsion loading (component σ_5) provides a value of 1.75.

Two short FE computations have to be made to calibrate the model parameters. Assuming that direction 1 is normal to the notch root and direction 2 is the tensile direction, a tension loading allows to define the components 22, 23, 33 of the tensors. A torsion test is needed to calibrate the components 55. These two sets of parameters are calibrated separately. For this purpose, FE computations are considered as a "numerical experiment", and the parameters of the simplified model are adjusted to reproduce the same curve. Once the parameters are adjusted, they can be used to simulate a very large number of cycles.

The full specimen is modeled by second order tetrahedral solid elements with reduced integration (10 nodes, 5 Gauss points) for computing the random non-proportional loading.

The mesh is presented in figure 2. A convergence has been made to establish the relevant element size at the notch root. The value for the final mesh is 0.14 mm i.e. 1.5 % of the core diameter. The FE results were read at the notch tip, on the x_1 axis.

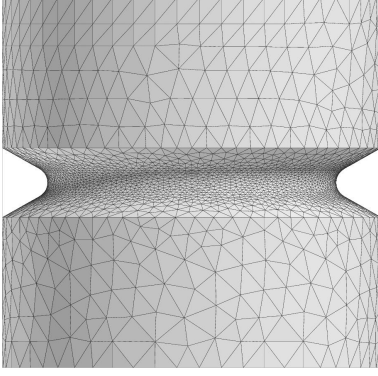


Figure 2: Mesh for the random multiaxial loading: 60905 elements, 267807 dof

C_{22}^N	$1.22 \cdot 10^5$ MPa	D_{22}^N	$1.45 \cdot 10^1$
C_{33}^N	$2.14 \cdot 10^5$ MPa	D_{33}^N	$7.72 \cdot 10^2$
C_{23}^N	$4.02 \cdot 10^4$ MPa	D_{23}^N	$6.64 \cdot 10^1$
C_{55}^N	$6.17 \cdot 10^4$ MPa	D_{55}^N	$3.81 \cdot 10^2$
δ	0.92		

Table 1: The parameters of the N-type correction, obtained by calibration on pure tensile and pure shear tests [9]

In the FEA (mesh of figure 2), the bottom of the specimen is fixed in all directions. A tensile force and a torsion force are applied on the top of the mesh. At the notch root, there are several non zero terms in the stress and strain tensors, namely $\sigma_2 = \sigma_{22}$, $\sigma_3 = \sigma_{33}$ and $\sigma_5 = \sigma_{23}$, $\varepsilon_1 = \varepsilon_{11}$, $\varepsilon_2 = \varepsilon_{22}$, $\varepsilon_3 = \varepsilon_{33}$ and $\varepsilon_5 = \varepsilon_{23}$. The model parameters of the N-type correction have been identified on the first three branches of two tension and torsion loadings, even if they could have been calibrated on any combined loading. They are presented in table 1.

This model has been applied to a series of tests with various ratios, various loading levels and loadings types. In each case, the predictions are in good agreement with the reference provided by FEA [9].

4.1 Predicted local stress-strain histories

The present paper focuses on multiaxial nonproportional random loading. The loading history is given in figure 3. The comparisons of the N-type rule and the FEA are given in figure 4. Once again, the model gives a rather good approximation. The results of our model are quite superposed with the signals provided by the finite element method, except for ε_3 , which values are very low. Buczynski-Glinka's method cannot be applied here, since it requires a signal preprocessing [8] that cannot be applied if the principal directions change.

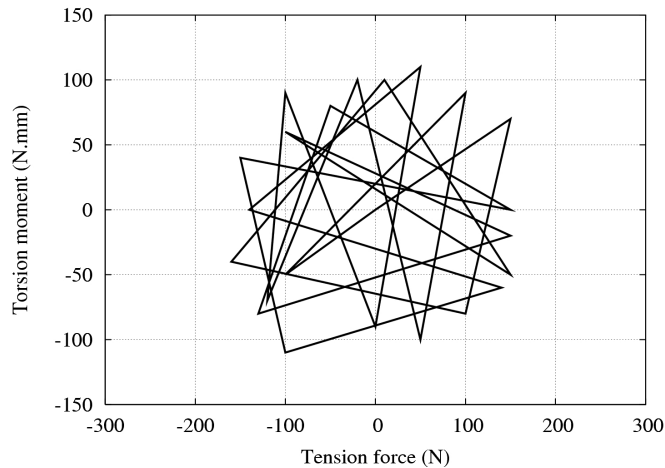


Figure 3: Random multiaxial non-proportional loadpath

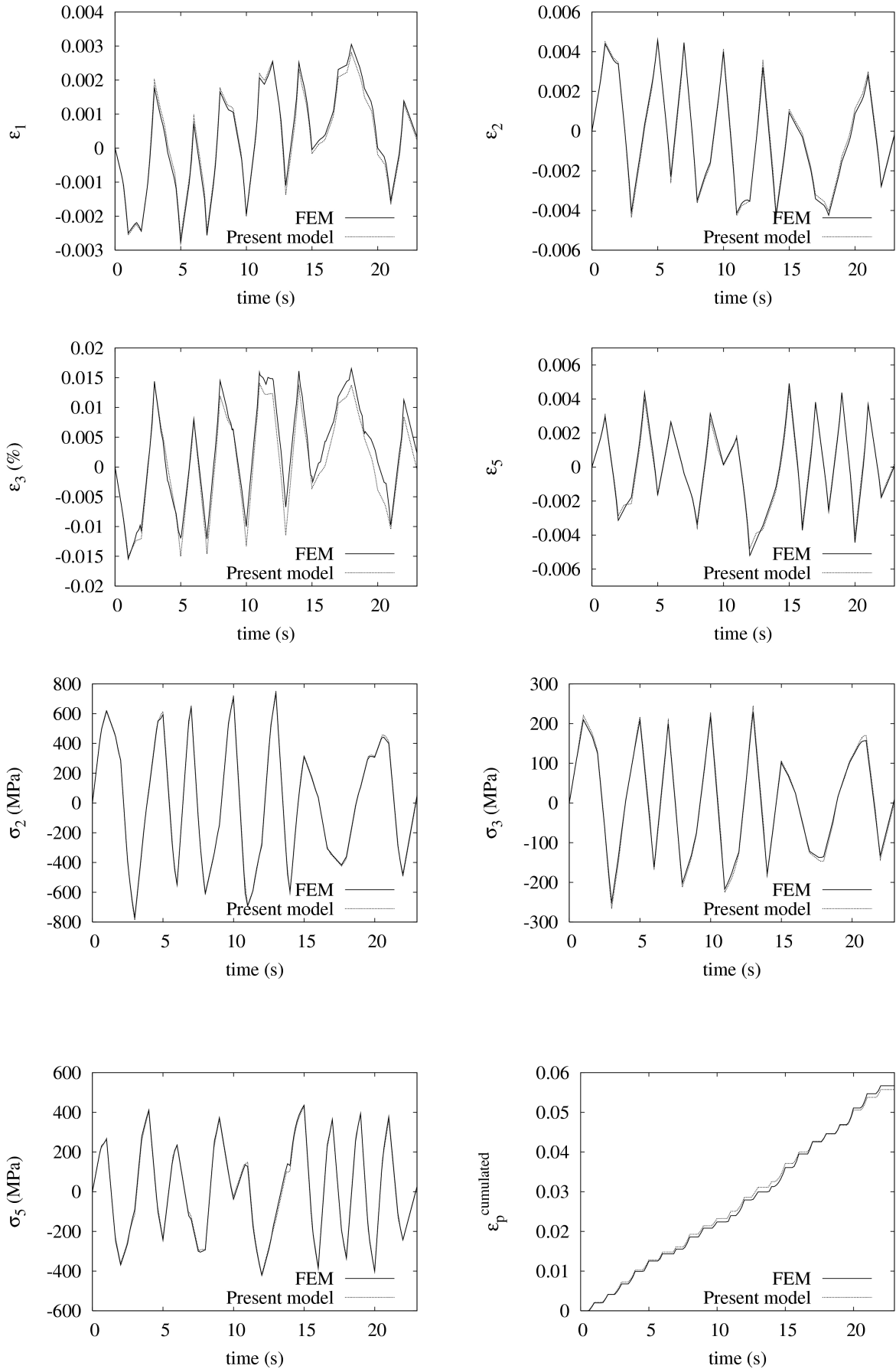


Figure 4: Comparison of the local histories obtained by FEA and the present model for a random non-proportional loading

4.2 Predicted fatigue life

The fatigue properties of 30CrNiMo8 have been identified on a S-N curve at $R = -1$. The following parameters have been calibrated:

$$M = 20860 \text{ MPa} \quad \beta = 2.87 \quad \sigma_l = 584 \text{ MPa} \quad \sigma_u = 1153 \text{ MPa} \quad a = 1$$

The local stress-strain histories computed at the notch tip by FEM and evaluated by the present model are used as an input of the multiaxial rainflow algorithm. In both cases, 13 cycles have been extracted. These cycles are used to predict the fatigue life of the specimen. We predict the fracture of the specimen after:

- 1452 realisations of the signal by using the histories computed by FEM;
- 1404 realisations of the signal by using the histories computed by the N-type correction.

The predicted fatigue lives calculated after the finite element computation and after the N-type correction are very close to each other.

5 CONCLUDING REMARKS

In this study, we presented an accelerated computation method based on a new approach. An adjustable elasto-plastic correction rule is used to compute the local stresses and strains at the notch root. Two types of corrections –namely L- and N-type– are used respectively in case of constant or variable amplitude loadings. The new method has been validated under a random non-proportional loading applied to an axisymmetric notched specimen. The results of our model are quite close to the finite element results, even in the hoop direction, where most of the existing methods fail. Moreover, among the existing accelerated computation methods, our model is the only one that can be applied to random non-proportional loadings. These results are quite encouraging, and show that this method can be used as a preprocessor for a multiaxial fatigue analysis.

Further studies will focus on the physical meaning of the model parameters. We will try to develop an expression of the parameters as a function of :

- the geometry, implying stress concentration factors matrixes;
- the behaviour, by means of the parameters of the constitutive equations.

Such a rule would avoid new identifications of the L- or N-type correction parameters. Also, it is worth noting that the impact of the errors made by each accelerated method on the fatigue life prediction accuracy strongly depends on the fatigue model that is used. Thus, other fatigue models will be further applied.

References

- [1] M.E. Barkey, D.F. Socie, and K.J. Hsia. A yield surface approach to the estimation of notch strains for proportional and nonproportional cyclic loading. *J. of Engng. Mat. Technol.*, 116:173–180, 1994.
- [2] M. Berveiller and A. Zaoui. An extension of the self-consistent scheme to plastically flowing polycrystal. *J. Mech. Phys. Sol.*, 26:325–344, 1979.
- [3] J. Besson, R. Le Riche, R. Foerch, and G. Cailletaud. Object-oriented programming applied to the finite element method. Part II: Application to material behaviors. *Revue Européenne des Éléments Finis*, 7(5):567–588, 1998.

- [4] M. Blétry and Cailletaud G. *Fatigue des Matériaux et des structures III*, chapter 7 : Fatigue multiaxiale. A. Pineau and C. Bathias editors, Hermès, 2009.
- [5] A. Buczynski and G. Glinka. An analysis of elasto-plastic strains and stresses in notched bodies subjected to cyclic non-proportional loading paths. *Biaxial/Multiaxial Fatigue and Fracture*, pages 265–283, 2003.
- [6] G. Cailletaud. *Une approche micromécanique phénoménologique du comportement inélastique des métaux*. PhD thesis, Université Pierre et Marie Curie, Paris 6, 1987.
- [7] G. Cailletaud and P. Pilvin. Utilisation de modèles polycristallins pour le calcul par éléments finis. *Revue Européenne des Éléments Finis*, 3(4):515–541, 1994.
- [8] C.-C. Chu and F.A. Conle. Multiaxial Neuber-type of elastic to elastic-plastic stress-strain correction. *Proceedings of the 4th Int. Conf. on Biaxial/Multiaxial Fatigue, Paris, France, 1994*.
- [9] T. Herbland, G. Cailletaud, S. Quilici, and H. Jaffal. Accelerated computation of local stress and strain states at notch root under multiaxial random loadings. *Submitted*, 2009.
- [10] R. Hill. A self-consistent mechanics of composite materials. *J. Mech. Phys. Sol.*, 13:213–222, 1965.
- [11] M. Hoffmann and T. Seeger. A generalized method for estimating multiaxial elastic-plastic notch stresses and strains. *Fatigue and Fracture of Engng Mat and Struct*, 107:250–260, 1985.
- [12] E. Kröner. Zur plastischen Verformung des Vielkristalls. *Acta Metall.*, 9:155–161, 1961.
- [13] J. Lemaitre and J. L. Chaboche. *Mécanique des Matériaux Solides*. Dunod, 1985.
- [14] J. Lemaitre and J.L. Chaboche. Aspect phénoménologique de la rupture par endommagement. *J. de mécanique appliquée*, 2(3):317–365, 1978.
- [15] B.E. Melnikov and A.S. Semenov. Multisurface theory of plasticity with one active surface. *Zeitschrift fr angewandte Mathematik und Mechanik*, 78:615–616, 1998.
- [16] A. Moftakhar, A. Buczynski, and G. Glinka. Calculation of elasto-plastic strains and stresses in notches under multiaxial loading. *Int. J. Frac*, 70:357–373, 1995.
- [17] H. Neuber. Theory of stress concentration for shear-strained prismatical bodies with arbitrary nonlinear stress-strain law. *J. of Applied Mechanics*, pages 544–550, 1961.
- [18] S. Quilici and A. Musienko. Calcul de durées de vie en fatigue HCF avec le modèle ONERA, application à un spectre d’accélération de type Carlos. Technical report, MINES-ParisTech, October 2004.
- [19] K. Sai, G. Cailletaud, and S. Forest. Micro-mechanical modeling of the inelastic behavior of directionally solidified materials. *Mech. of Materials*, 38:203–217, 2006.